Analysis of Debonding along Interface of AA4015/Magnesium Oxide Nanoparticulate Reinforced Metal Matrix Composites

[1]P. M. Jebaraj and A. Chennakesava Reddy[2]

[1]Professor, Department of Mechanical Engineering, Dr. Ambedkar Institute of Technology, Bangalore, India
[2]Assistant Professor, Department of Mechanical Engineering, MJ College of Engineering and Technology, Hyderabad, India
dr_acreddy@yahoo.com

Abstract: A hexagonal array unit cell/2-D rhombus particulate RVE models were employed to evaluate interfacial debonding using cohesive zone analysis. The particulate metal matrix composites are magnesium oxide/AA4015 alloy at volume fractions of 10%, 20% and 30% magnesium oxide. Interface debonding was observed in all the composites. The normal traction in the region of interface between MgO nanoparticulate and AA4015 alloy matrix has decreased with increase of volume fraction of MgO.

Keywords: AA4015 alloy, magnesium oxide, rhombus particulate, RVE model, finite element analysis, interface debonding.

1. INTRODUCTION

The interface between the inclusion and the matrix is a bonding surface, across which both weak and strong discontinuities occur [1]. In particular, the overall bulk strength of the composite depends strongly on interfacial damage and debonding. The overall performance of a composite depends on the material properties of each phase as well as the interfacial properties between the matrix and inclusions. Interfacial decohesion is usually observed in composites with very low strength matrices relative to the inclusion while particle fracture usually occurs with a medium to high strength matrix [2]. The interfacial zone has been modeled in a number of ways, including as a narrow region of continuum with graded properties, as an infinitely thin surface with springs, and as a cohesive zone with traction-separation relations. Recently, the cohesive zone approach has become widely used. one of the first to apply the traction-separation cohesive relationship to the model [3]. Several research papers were focused to predict interfacial damage of the composite using representative volume element models and finite element methods [4-17].

The current research was to develop a 2D simulation capability of interfacial decohesion of a particulate-reinforced composite material of AA4015/magnesium oxide. Representative volume elements (RVEs) models were taken from the periodic 2-D rhombus particulates in a hexagonal array distribution (figure 1).

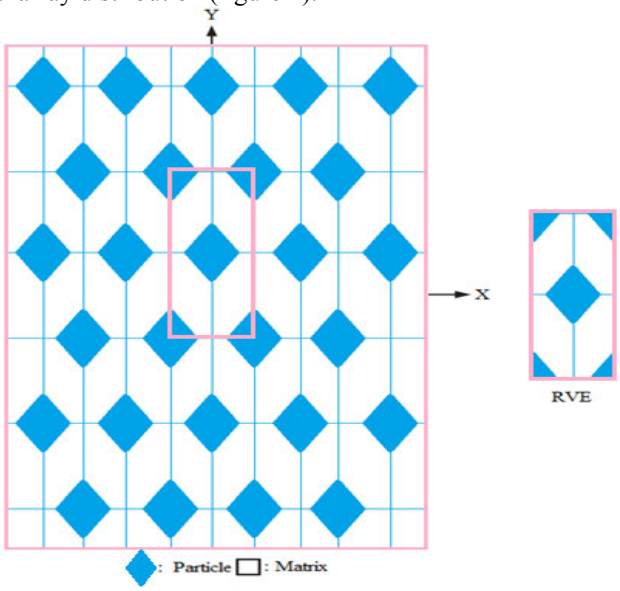

Figure 1: The RVE model.

2. MATERIALS AND METHODS

The computational domain considered in the current research is comprised of AA4015alloy matrix material with an embedded 2-D rhombus magnesium oxide inclusion. The volume fractions of magnesium oxide (MgO) were 10%, 20%, and 30%. PLANE183 element was used for the matrix and the nanoparticulates. The cohesive zone can be incorporated in the continuum formulation by applying the cohesive tractions as boundary conditions. The cohesive element is implemented as a linear element with four nodes. Initially, the interface between the matrix material and the inclusion is assumed to be perfectly bonded, that is, continuity of traction and displacement is assumed along the interface. The finite element analysis was carried out for the single inclusion model undergoing a tensile load. The elastic material properties are given by E_m = 68.90 GPa, E_p = 270 GPa, ν_m = 0.34 and ν_p = 0.35.

Shear-log model is based on the assumption that all of the load transfer from matrix to particulate occurs via shear stresses acting on the particulate interface between the two constituents. The rate of change of the stress in the particulate to the interfacial shear stress at that point and the particulate radius, 'r' is given by:

$$\frac{d\sigma_p}{dx} = -\frac{2\tau_i}{r} \quad (1)$$

which may be regarded as the basic shear lag relationship.

The stress distribution in the particulate is determined by relating shear strains in the matrix around the particulate to the macroscopic strain of the composite. Some mathematical manipulation leads to a solution for the distribution of stress at a distance 'x' from the mid-point of the particulate which involves hyperbolic trig functions:

$$\sigma_p = E_p\varepsilon_c[1 - cosh(nx/r)sech(ns)] \quad (2)$$

where ε_c is the composite strain, s is the particulate aspect ratio (length/diameter) and n is a dimensionless constant given by:

$$n = \left[\frac{2E_m}{E_p(1+\nu_m)ln(1+\nu_p)}\right]^{1/2} \quad (3)$$

in which ν_m is the Poisson ratio of the matrix. The variation of interfacial shear stress along the particulate length is derived, according to Equation (1), by differentiating this equation, to give:

$$\tau_i = \frac{n\varepsilon_c}{2}E_p sinh\left(\frac{nx}{r}\right)sech(ns) \quad (4)$$

The equation for the stress in the particulate, together with the assumption of a average tensile strain in the matrix equal to that imposed on the composite, can be used to evaluate the composite stiffness. This leads to:

$$\sigma_c = \varepsilon_c\left[\nu_p E_p\left(1 - \frac{tanh(ns)}{ns}\right) + (1-\nu_p)E_m\right] \quad (5)$$

The expression in square brackets is the composite stiffness. The stiffness is a function of particulate aspect ratio, particulate/matrix stiffness ratio and particulate volume fraction.

If the particle deforms in an elastic manner (according to Hooke's law) then,

$$\tau = \frac{n}{2}\sigma_p \quad (6)$$

If interfacial debonding/yielding is considered to occur when the interfacial shear stress reaches its shear strength

$$\tau = \tau_{max} \quad (7)$$

For particle/matrix interfacial fracture can be established whereby,

$$\tau_{max} < \frac{n\sigma_p}{2} \quad (8)$$

This approach suggests that the outcome of a matrix crack impinging on an embedded particle depends on the balance between the particle strength and the shear strength of the interface. For plane strain conditions, the macro stress- macro strain relation is as follows:

$$\begin{Bmatrix}\overline{\sigma_x}\\ \overline{\sigma_y}\\ \overline{\tau_{xy}}\end{Bmatrix} = \begin{bmatrix}\overline{C_{11}} & \overline{C_{12}} & 0\\ \overline{C_{21}} & \overline{C_{22}} & 0\\ 0 & 0 & \overline{C_{33}}\end{bmatrix} \times \begin{Bmatrix}\overline{\varepsilon_x}\\ \overline{\varepsilon_y}\\ \overline{\gamma_{xy}}\end{Bmatrix} \quad (9)$$

The interfacial tractions can be obtained by transforming the micro stresses at the interface as given in Eq. (3):

$$t = \begin{Bmatrix}t_z\\ t_n\\ t_t\end{Bmatrix} = T\sigma \quad (10)$$

where, $T = \begin{bmatrix}0 & 0 & 0\\ cos^2\theta & sin^2\theta & 2sin\theta cos\theta\\ -sin\theta cos\theta & sin\theta cos\theta & cos^2\theta - sin^2\theta\end{bmatrix}$

3. RESULTS AND DISCUSSION

The tensile modulus and compressive modulus decreased with volume fraction of MgO as shown figure 2a. The shear modulus also decreased with increase in the volume fraction of MgO in the composites (figure 2b). The major Poisson's ratio was highest for 20% MgO. The stiffness mismatch between MgO nanoparticulate and AA4015 alloy matrix is 201,10 GPa. The condition $\tau_{max} < n\sigma_p/2$ is satisfied for the incidence of debonding in the composites including 10%, 20% and 30% MgO (figure 3). The shear stresses induced in the composites are shown in figure 4. For the shearing of interface between the MgO inclusion and AA4015 alloy matrix, the shear stress decreased with increase of MgO inclusion in AA4015 alloy matrix.

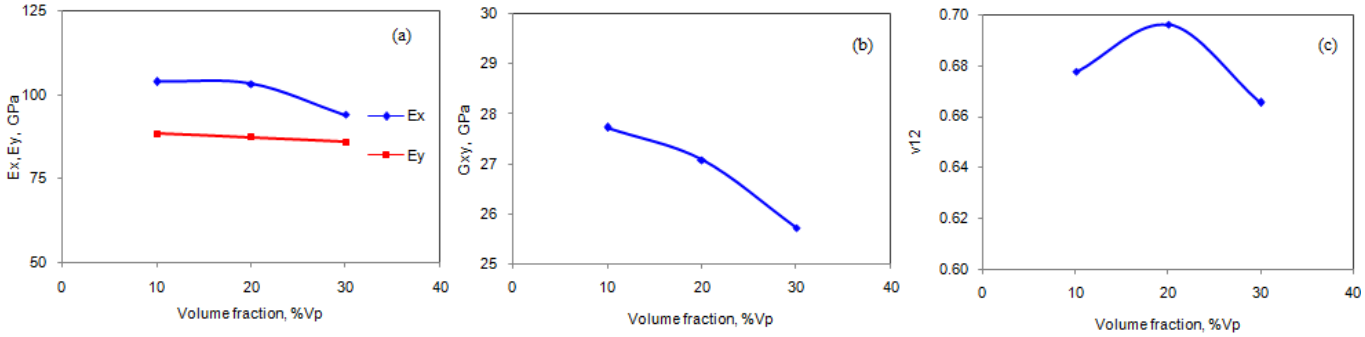

Figure 2: Effect of volume fraction on effective material properties.

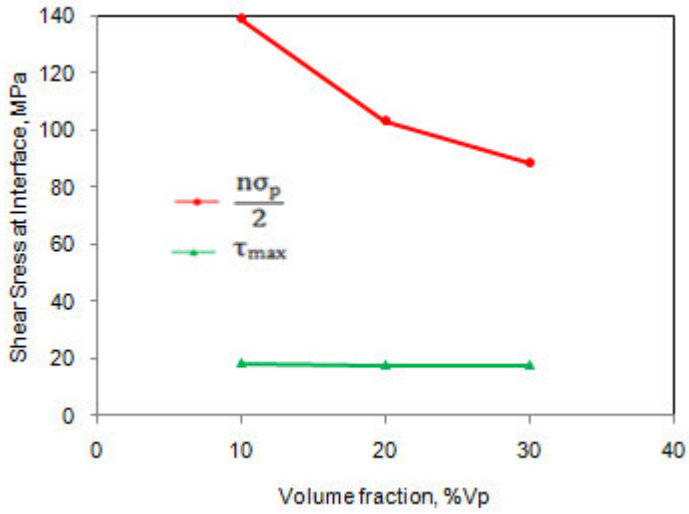

Figure 3: Fracture criteria of interface debonding.

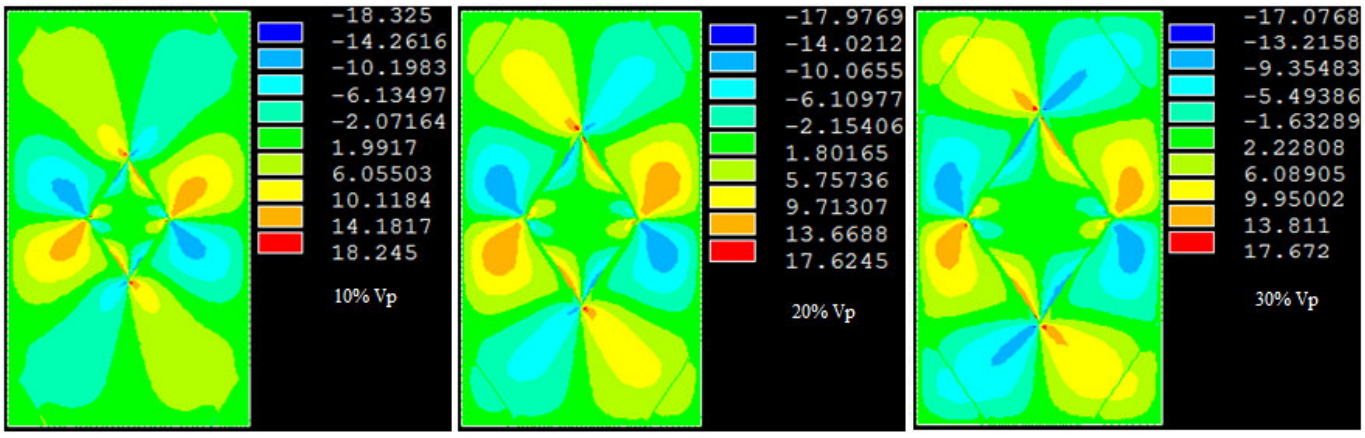

Figure 4: Effect of volume fraction on shear strength.

The normal and tangential tractions are plotted in figure 5a. Because of symmetry considerations, the variations of the interface stresses with circumferential location are plotted only for the range $0^o \leq \theta \leq 90^o$. The normal traction in the region of interface between MgO nanoparticulate and AA4015 alloy matrix has decreased with increase of volume fraction of MgO. Although the plots shown are for the normal traction dominated failure, the results for the tangential traction dominated failure are qualitatively similar. Once a portion of the interface becomes partially debonded, the damage zone slides tangentially along the interface until a compressive region is reached. The normal and tangential displacements are also plotted in figure 5b. There is clear indication of dependence of interface tractions on interfacial separation.

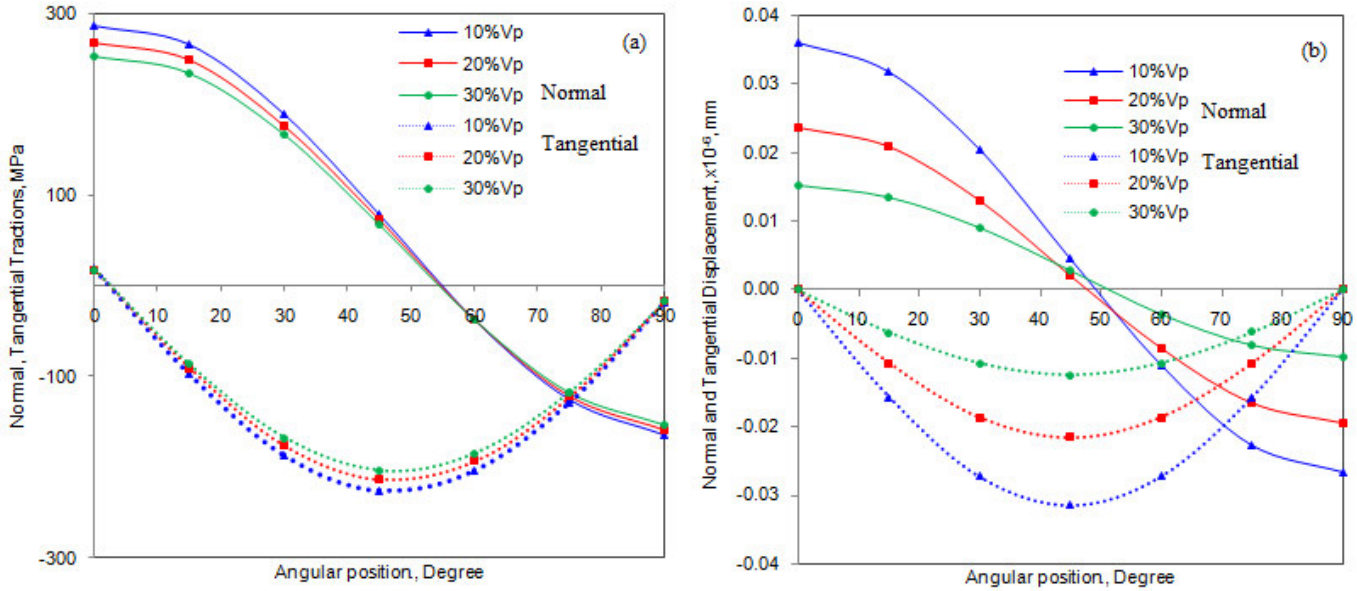

Figure 5: Normal and tangential: (a) tractions and (b) displacements.

4. CONCLUSION

The interface debonding occurred in the composites containing 10%, 20% and 30% volume fractions MgO. The normal traction in the region of interface between MgO nanoparticulate and AA4015 alloy matrix has decreased with increase of volume fraction of MgO. The damage zone slides tangentially along the interface until a compressive region is reached.

REFERENCES

1. K. K. Chawla, Composite Materials Science and Engineering, Springer Science Business, New York, 1998.
2. A. F. Whitehouse, T. W. Clyne, Cavity formation during tensile straining of particulate and short fiber metal-matrix composites, Acta Met. Mat. 41 (6), 1993, pp.1701–1711.
3. A. Needleman, An analysis of decohesion along an imperfect interface. International Journal of Fracture, 42, 1990, pp. 21-40.
4. A. Chennakesava Reddy, Assessment of Debonding and Particulate Fracture Occurrences in Circular Silicon Nitride Particulate/AA5050 Alloy Metal Matrix Composites , National Conference on Materials and Manufacturing Processes, Hyderabad, India, 27-28 February1998, pp.104-109.
5. B. Kotiveera Chari and A. Chennakesava Reddy, Numerical Simulation of Particulate Fracture in Round Silicon Nitride Particulate/AA6061 Alloy Metal Matrix Composites, National Conference on Materials and Manufacturing Processes, Hyderabad, India, 27-28 February 1998, pp. 110-114.
6. H. B. Niranjan and A. Chennakesava Reddy, Effect of Elastic Moduli Mismatch on Particulate Fracture in AA7020/Silicon Nitride Particulate Metal Matrix Composites , National Conference on Materials and Manufacturing Processes, Hyderabad, India, 27-28 February, 1998, pp. 115-118,
7. P. Martin Jebaraj and A. Chennakesava Reddy, Cohesive Zone Modelling for Interface Debonding in AA8090/Silicon Nitride Nanoparticulate Metal Matrix Composites, National Conference on Materials and Manufacturing Processes, Hyderabad, India, 27-28 February 1998, pp. 119-122.
8. P. Martin Jebaraj and A. Chennakesava Reddy, Plane Strain Finite Element Modeling for Interface Debonding in AA1100/Silicon Oxide Nanoparticulate Metal Matrix Composites, National Conference on Materials and Manufacturing Processes, Hyderabad, India, 27-28 February 1998, pp. 123-126.
9. A. Chennakesava Reddy, Local Stress Differential for Particulate Fracture in AA2024/Titanium Carbide Nanoparticulate Metal Matrix Composites, National Conference on Materials and Manufacturing Processes, Hyderabad, India, 27-28 February 1998, pp. 127-131.

10. B. Kotiveera Chari and A. Chennakesava Reddy, Interface Debonding and Particulate Facture based on Strain Energy Density in AA3003/MgO Nanoparticulate Metal Matrix Composites, National Conference on Materials and Manufacturing Processes, Hyderabad, India, 27-28 February 1998, pp. 132-136.
11. H. B. Niranjan and A. Chennakesava Reddy, Numerical and Analytical Prediction of Interface Debonding in AA4015/Boron Nitride Nanoparticulate Metal Matrix Composites , National Conference on Materials and Manufacturing Processes, Hyderabad, India, 27-28 February 1998, pp. 137-140.
12. S. Sundara Rajan and A. Chennakesava Reddy, Effect of Particulate Volume Fraction on Particulate Cracking in AA5050/Zirconium Oxide Nanoparticulate Metal Matrix Composites , National Conference on Materials and Manufacturing Processes, Hyderabad, India, 27-28 February 1998, pp. 156-159.
13. S. Sundara Rajan and A. Chennakesava Reddy, Cohesive Zone Analysis for Interface Debonding in AA6061/Titanium Nitride Nanoparticulate Metal Matrix Composites , National Conference on Materials and Manufacturing Processes, Hyderabad, India, 27-28 February 1998, pp. 160-164.
14. A. Chennakesava Reddy, Effect of Particle Loading on Microealstic Behavior and interfacial Tractions of Boron Carbide/AA4015 Alloy Metal Matrix Composites, 1st International Conference on Composite Materials and Characterization, Bangalore, 14-15 march 1997, pp. 176-179.7
15. A. Chennakesava Reddy, Reckoning of Micro-stresses and interfacial Tractions in Titanium Boride/AA2024 Alloy Metal Matrix Composites, 1st International Conference on Composite Materials and Characterization, Bangalore, 14-15 march 1997, pp. 195-197.
16. A. Chennakesava Reddy, Interfacial Debonding Analysis in Terms of Interfacial Tractions for Titanium Boride/AA3003 Alloy Metal Matrix Composites, 1st National Conference on Modern Materials and Manufacturing , Pune, India, 19-20 December 1997, pp. 124-127.
17. A. Chennakesava Reddy, Evaluation of Debonding and Dislocation Occurrences in Rhombus Silicon Nitride Particulate/AA4015 Alloy Metal Matrix Composites, 1st National Conference on Modern Materials and Manufacturing , Pune, India, 19-20 December 1997, pp. 278-282.